Journal of Nano- and Electronic Physics
Vol. **16** No 5, 05020(6pp) (2024)

Журнал нано- та електронної фізики
Том **16** № 5, 05020(6cc) (2024)

OPEN ACCESS

REGULAR ARTICLE

Novel Synthesis and Structural Study of Cadmium Doped Cobalt Ferrite Nanoparticles through X-ray Diffraction Analysis

Priyanka P. Kashid[1,2], Shridhar N. Mathad[1,2,*], Rakesh M. Shedam[1,2], Mahadev Shedam[3]

[1] *Department of Engineering Physics, K.L.E. Institute of Technology, Gokul Road, Hubballi, 580027 Karnataka, India*
[2] *Visvesvaraya Technological University (VTU), 590018 Belagavi, India*
[3] *The New College, Kolhapur, India*

(Received 15 June 2024; revised manuscript received 22 October 2024; published online 30 October 2024)

This paper investigated the structural properties of nano-crystalline Cd^{2+} doped cobalt ferrite ($Co_{1-x}Cd_xFe_2O_4$) nanoparticles were synthesized by co-precipitation method. X-ray diffraction study revealed the formation of mono phase cubic spinels. The crystallite size was found to be increased from 17 to 38 nm with increase of cadmium concentration. The other structural parameters like lattice constant (a), volume (V), hopping lengths (L_A and L_B), bond lengths (A-O and B-O), ionic radii (r_A and r_B), X-ray density (D_x), microstrain (ε) and dislocation density (ρ_D) were also estimated. Here, *W-H* and Size-Strain Plot methods were used for obtaining the values of lattice strain and crystallite size from the X-ray diffraction peak broadening analysis. Each method of analysis was different result because, the variation was found in calculated parameters.

Keywords: Microstrain (ε), Crystallite size (D), X-ray density (D_x), Ferrite nanoparticles, Cd^{2+} substitution.

DOI: 10.21272/jnep.16(5).05020 PACS numbers: 68.37.Hk, 81.20.Ka

1. INTRODUCTION

In past decades, nanotechnology has received a great attention of researchers. It involves the ability to control the human designed working devices. Today's engineers and scientists are searching number of roots to synthesis the materials at nano and pico scale, having huge advantages with excellent properties such as, lighter weight, higher strength, greater chemical reactivity, increased control of light spectrum and smaller size [1]. With such advent in nanotechnology and synthesis of nanomaterials have taken a revolutionary way in the form of magnetic nanoparticles particularly, ferrite nanoparticles with their spectacular properties and innovative applications.

Cobalt ferrite ($CoFe_2O_4$) has achieved a distinct attention in research because of its extensive applications in permanent magnets, high storage devices, magnetic resonance imaging (MRI), microwave devices, magnetic fluid, drug delivery, catalysis, gas sensors, telecommunication equipments, information storage media, and hybrid super capacitors [2-3]. Recent research has focused on the synthesis and characterization of cobalt ferrite nanoparticles with controlled size, shape, and surface properties for improved performance in various biomedical applications. Various synthesis methods, such as sol-gel, co-precipitation, hydrothermal, and microwave-assisted synthesis, have been employed to produce cobalt ferrite nanoparticles with tunable properties [4]. The unique magnetic properties of cobalt ferrite nanoparticles, such as high magnetic anisotropy and superparamagnetism, make them attractive for magnetic hyperthermia applications, where they can be used to selectively heat cancer cells and induce cell death. In addition, cobalt ferrite nanoparticles have been explored as MRI contrast agents due to their high magnetic moment and relaxivity [5-7]. Cobalt ferrite nanoparticles have also shown promise as drug delivery vehicles for cancer therapy. The high surface area and unique surface chemistry of these nanoparticles enable them to adsorb and deliver drugs to specific target sites. Furthermore, the magnetic properties of cobalt ferrite nanoparticles allow for their targeted delivery and controlled release under the influence of an external magnetic field [8-9]. The magnetic properties of cobalt ferrite have led to its use in magnetic nanoparticles for biomedical applications, such as magnetic hyperthermia, MRI contrast agents, and drug delivery systems. Magnetic hyperthermia is a promising cancer therapy technique that involves the targeted heating of cancer cells using magnetic nanoparticles under the influence of an external magnetic field. The unique magnetic properties of cobalt ferrite, including high magnetic anisotropy and superparamagnetism, make it an ideal candidate for magnetic hyperthermia applications [10-11]. In, inverse spinel structure of cobalt ferrite, one half of Fe^{3+} ions are occupying tetrahedral (A) sites and rest half of Fe^{3+} ions with Co^{2+} ions are located at octahedral (B) sites [12]. Along with this, the properties of cobalt ferrite can be enhanced by various chemical modifications such as preparation methods, substituting one or more guest metal

* Correspondence e-mail: physicssiddu@kleit.ac.in

Cite this article as: P.P. Kashid et al., *J. Nano- Electron. Phys.* 16 No 5, 05020 (2024) https://doi.org/10.21272/jnep.16(5).05020

ions into host lattice, modifying the reaction conditions, etc. To best of our knowledge, few investigations were reported on Cd substituted Co ferrite nanoparticles. In details, Reddy et al., presented the magnetic properties of $Cd_{0.5}Co_{0.5}Fe_2O_4$ ferrites and their results revealed that Cd dopant plays an important role in modification of the saturation magnetization, coercivity and remanence magnetization. The lower coercivity exhibits super paramagnetic behavior of synthesized ferrites [13]. Abdeen et al, reported that the structural parameters like X-ray density, lattice parameter and ionic radius at tetrahedral site show an increasing trend with increase of Cd content. The activation energy for mobility (E_μ) was found to be very close to the activation energy for conduction process ($E_{\sigma T}$) results the presence of hopping conduction mechanism in prepared ferrite samples [14].

The present work demonstrates, the novel synthesis and structural behavior of cadmium doped cobalt ferrite; which have been prepared by co-precipitation root. The structural properties of desired nanoparticles analyzed thoroughly the Williamson-Hall (W-H) and Size-strain plot methods. Afterthat, various structural parameters like crystallite size, microstrain, lattice parameter, hopping length, ionic radii, bond length, dislocation density were calculated using standard formulae.

2. EXPERIMENTAL DETAILS

The $Co_{1-x}Cd_xFe_2O_4$ (x = 0.08, 0.16, 0.24, 0.32, 0.40 and 0.48) nanoparticles were synthesized via coprecipitation method. First, the stoichiometric amount of precursors like $CoCl_2.6H_2O$ (≥ 98 % pure, Sigma Aldrich), $CdCl_2.H_2O$ (≥ 98 %, pure, Sigma Aldrich) and $FeCl_3.6H_2O$ (≥ 99 %, pure, Sigma Aldrich) were dissolved in 100 ml of distilled water separately. All solutions were mixed with continuous stirring at 60 °C for half hour. The sodium hydroxide (NaOH) was added dropwise until the precipitation was completed at pH of around 8.The obtained co-precipitation product was filtered, and washed several times with distilled water. Then, precipitate was dried for 3 days at room temperature and was finely powdered using clean agate mortar. Finally, single phase spinel structure ferrite nanoparticles were formed by annealing the precipitates at 800 °C for 4 hours.

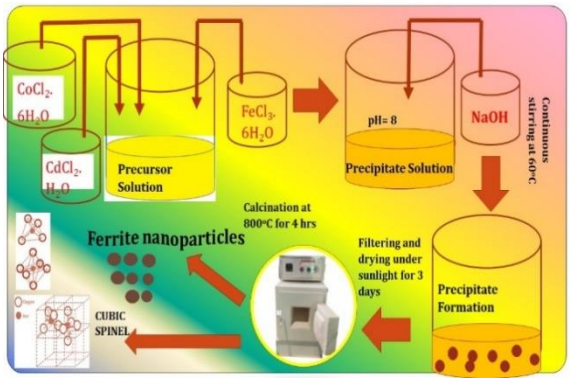

Fig. 1 – Schematic representation of Cd doped cobalt ferrite nanoparticles prepared by co- precipitation method

The present study was carried out the following outcomes:

1. The single phase formation of synthesized ferrite nanoparticles was confirmed by XRD analysis. X-ray diffraction patterns were obtained on Bruker D8 Advance diffractometer using Cu Kα radiation (λ = 1.5406 Å).
2. XRD peak broadening analysis was studied by using two dominant methods; the Williamson Hall model and the size-strain plot method.

These methods were given the nearly close values of crystallite size (D) and microstrain (ε) of respective ferrite compositions.

3. RESULTS AND DISCUSSION

3.1 X-ray Diffraction Analysis

X-ray diffraction spectra for $Co_{1-x}Cd_xFe_2O_4$ (x = 0.08, 0.16, 0.24, 0.32, 0.40 and 0.48) system sintered at 800 °C for 4 hours, are shown in Fig. 2. XRD results revealed that the synthesized samples are well crystallized into highly pure, mono phase, cubic spinels. For x = 0.08, the diffraction peaks are located at 2θ values of 18.21°, 29.91°, 35.40°, 36.99°, 42.97°, 53.43°, 56.97°, 62.56° corresponds to the (111), (220), (311), (222), (400), (422), (511) and (440) planes respectively. All these peak positions and intensities matched with cubic spinel lattice of standard $CoFe_2O_4$(JCPDS card #00-22-1086).

3.2 Crystallite Size and Lattice Parameter

The average crystallite size (D) of each synthesized sample is calculated from full width at half maximum (β) using Debye Scherrer equation [15].

$$D = \frac{0.9\lambda}{\beta \cos\theta} \tag{1}$$

Where, λ is wavelength of Cu-Kα radiation (1.54 Å), β is full width at half maximum (FWHM) and θ is the Bragg's angle.

The lattice parameter is determined by using the following relation [16].

$$a = \frac{d}{\sqrt{h^2 + k^2 + l^2}} \tag{2}$$

Where, d is an interplaner spacing and hkl are Miller indices. The increase of Cd^{2+} ion concentration, confirmed an increase in the lattice parameter from 8.4067 to 8.4416 Å. The crystallite size also found to be increased from 17.5 to 37.84 nm with Cdconcentration. The expansion in the lattice constant and crystallite size values is because of the replacement of smaller Co^{2+} ions 0.72 Å by larger Cd^{2+} ions 1.03 Å. This result is in good agreement with the previous reported result for $Co_{0.5}Cd_xFe_{2.5-x}O_4$ ferrites [17].

3.3 Hopping Length, Bond Length and Ionic Radius

The values of hopping lengths (L_A and L_B), bond lengths (A-O and B-O) and ionic radii (r_A and r_B) are determined by using following equations from eq. (3) to eq. (8).

$$L_A = \frac{a\sqrt{3}}{4} \tag{3}$$

$$L_B = \frac{a\sqrt{2}}{4} \quad (4)$$

Where, L_A and L_B are the distances (hopping lengths) between magnetic ions at (A) tetrahedral and (B) octahedral sites respectively. The hopping length values are found to be increased from 3.6402 to 3.6553 Å and 2.9722 to 2.9846 Å with increase of Cd^{2+} content. This may be due to the fact that, difference in ionic radii of constituent ions *i.e.* Cd^{2+} ion has higher ionic radius (1.03 Å) than that of Co^{2+} ion (0.72 Å). The bond lengths are calculated by using following relations.

$$A-O = \left(u-\frac{1}{4}\right)a\sqrt{3} \quad (5)$$

$$B-O = \left(\frac{5}{8}-u\right)a \quad (6)$$

Where, A-O is the inter-atomic distance i.e. tetrahedral bond length and B-O is the octahedral bond length. The bond lengths are increased from 1.8201 to 1.8277 Å and 2.1017 to 2.1104 Å with increase of Cd content. The following equations are used for determining the ionic radii values.

$$r_A = \left(u-\frac{1}{4}\right)a\sqrt{3} - r\left(O^{2-}\right) \quad (7)$$

$$r_B = \left(\frac{5}{8}-u\right)a - r\left(O^{2-}\right) \quad (8)$$

Where, $r(O^{2-})$ is the radius of an oxygen ion. Table 1. shows a slight increase in the ionic radii values at tetrahedral and at octahedral site respectively.

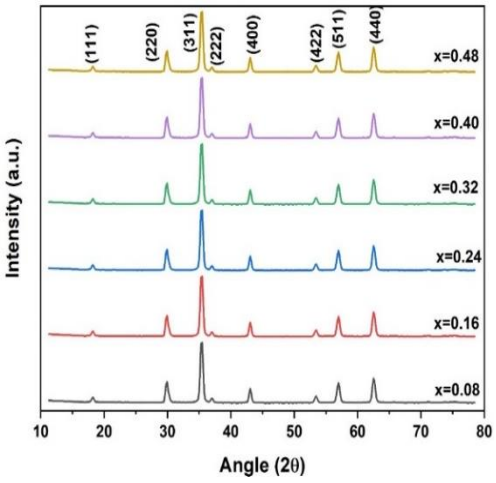

Fig. 2 – Powder X-ray diffraction patterns for $Co_{1-x}Cd_xFe_2O_4$ (x = 0.08, 0.16, 0.24, 0.32, 0.40, 0.48) nanoparticles

3.4 Volume of Unit Cell and X-ray Density

The concentration of Cd^{2+} ions increases, affirming an increase in the volume of unit cell from 594 to 601 m^3. This expansion can be explained on the basis of the ionic radius of the guest ions. The X-ray density of prepared samples is obtained by using following formula.

$$D_x = \frac{8M}{Na^3} \quad (9)$$

Where, M is the molecular weight of the corresponding composition and N is the Avogadro's no. From Table 1. It is clearly seen that the X-ray density slightly increases with increase of Cd content which should be due to the higher molecular weight of cadmium atom (112.41 g/mol) than that of the cobalt atom (58.93 g/mol). Though the lattice parameter increases, the increase in molar mass overtakes the increase in volume of prepared samples thus, the X-ray density increases. The replacement of such Co^{2+} ions by Cd^{2+} ions in prepared compositions lead to the variation in bond lengths and consequently in interatomic distances and densities. This increasing trend in volume and X-ray density is similar to those reported in previous literature [18].

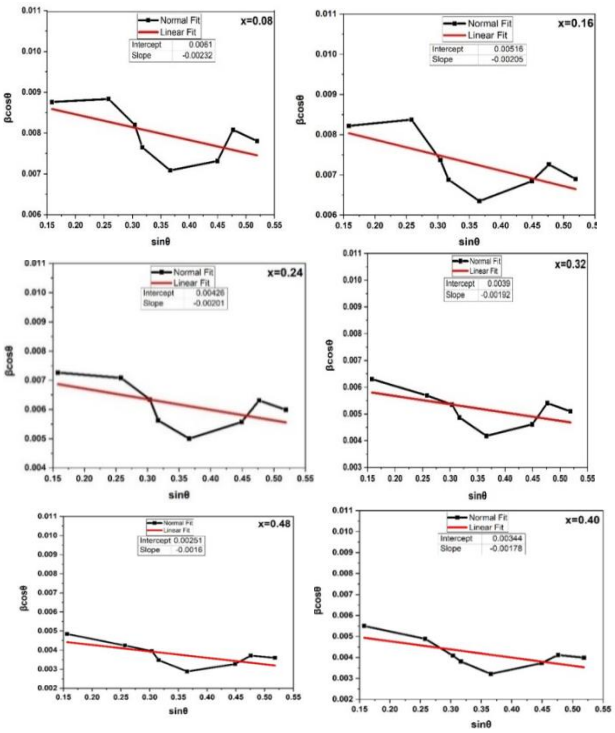

Fig. 3 – Williamson Hall plots for synthesized ferrite compositions

3.5 Williamson Hall Plot Method

Williamson and Hall suggested a method for obtaining the average crystallite size (D) and lattice strain (η) by using the following relation [19].

$$\frac{\beta\cos\theta}{\lambda} = \frac{1}{D} + \frac{\eta\sin\theta}{\lambda} \quad (10)$$

The above equation can also be present in the form of $y = mx + c$, where $m = \eta$ and $c = 1/D$. Thus, we get the lattice strain (η) from slope and crystallite size (D) from y-intercept by plotting a linear plot of $\beta\cos\theta$ *vs.* $\sin\theta$. By using Williamson Hall plot, the strain and crystallite size of various prepared compositions are calculated and are listed in Table 2. From *W-H* plots, it was seen that the crystallite size increased but the microstrain was decreased as Cd doping concentration increased.

Thus, we get the lattice strain (η) from slope and crystallite size (D) from y-intercept by plotting a linear plot of $\beta\cos\theta$ *vs.* $\sin\theta$. By using Williamson Hall plot, the strain and crystallite size of various prepared compositions are

calculated and are listed in Table 2. From *W-H* plots, it was seen that the crystallite size increased but the microstrain was decreased as Cd doping concentration increased.

3.6 Size-Strain Plot Method

In present method, the size strain parameters are obtained from the size-strain plot. The data from high angle reflections are given less importance i.e at high angles, X-ray diffraction peaks are highly overlapped so the data obtained is not good, where the precision is generally with low. Here, it is supposed that the crystallite size profile characterizes the Lorentzian function and the strain profile characterizes the Gaussian function. SSP measurements are calculated by using the following relation and the values are presented in Table 3 [20].

$$\left(d_{hkl}\beta_{hkl}\cos\theta\right)^2 = \frac{\kappa\lambda}{D}\left(d_{hkl}^2\beta_{hkl}\cos\theta\right) + \left(\frac{\varepsilon}{2}\right)^2 \qquad (11)$$

Where, K is the shape factor.

The Williamson Hall Plot method and stress-strain plots are essential tools in materials science and engineering which provides valuable insights into the behavior and properties of materials. Williamson Hall Plot method admits for the crystallite size (16-40 nm), micro-strain (4×10^{-3} to 5.8×10^{-3}) and SS Plots method allows for the determination of crystallite size(16-29 nm) and micro-strain (1.2×10^{-2} to 9×10^{-3}) in ferrite samples. Thus these analyses provide insights deep perception into the microstructural and mechanical properties of materials. Overall, the evaluated results and the extracted values of this study were in good agreement and Tabulated in Table 2.

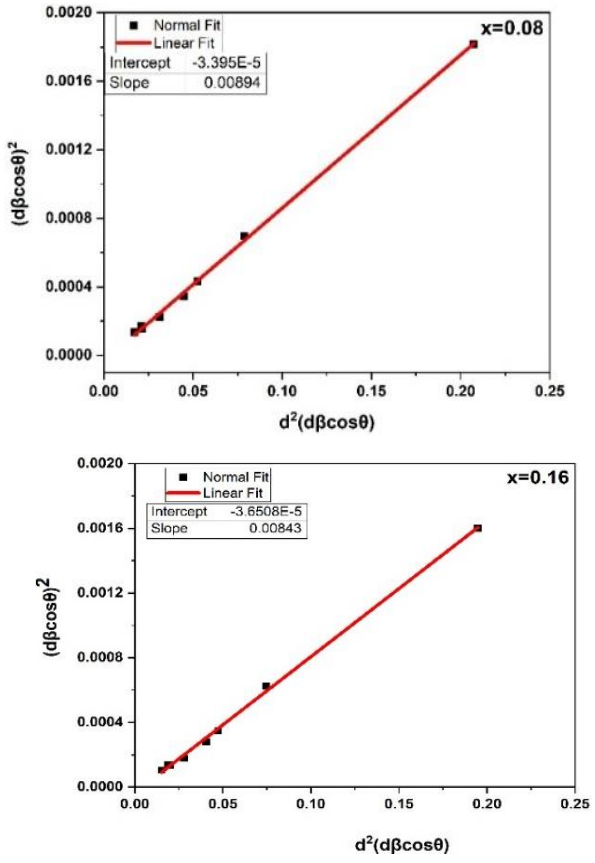

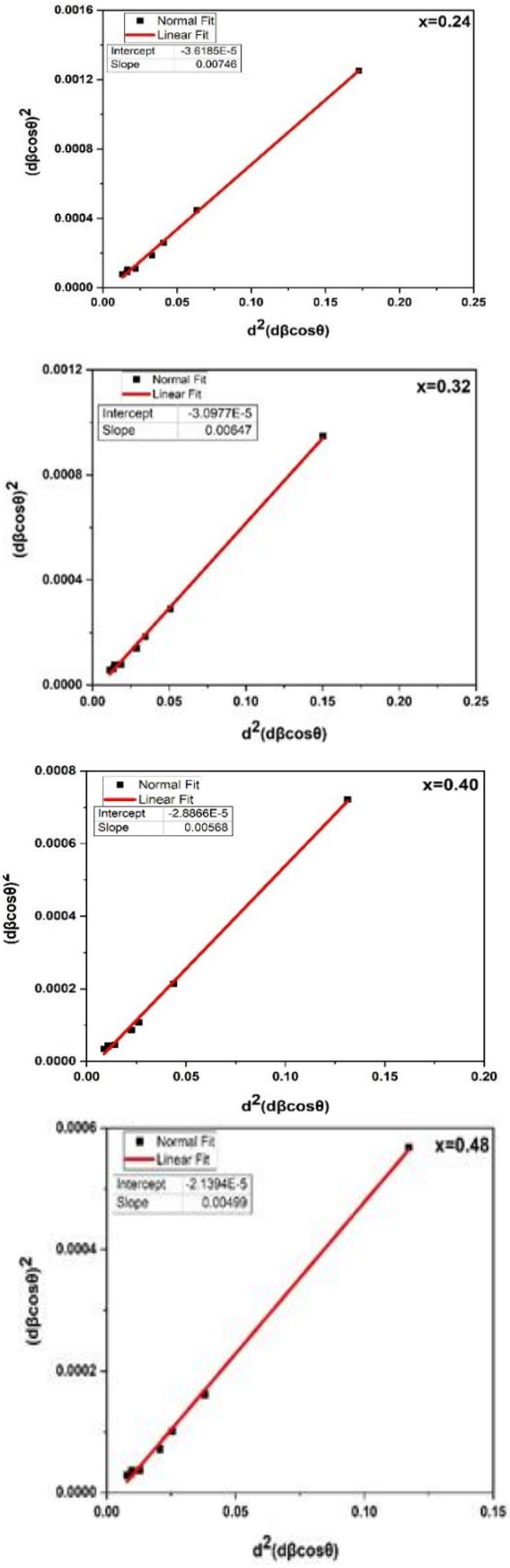

Fig.4 – Size-Strain plots for synthesized ferrite compositions (x = 0.08 to 0.48)

Table 1 – Various structural parameters for $Co_{1-x}Cd_xFe_2O_4$ nanoparticles

Parameters	0.08	0.16	0.24	0.32	0.40	0.48
Lattice constant a (Å)	8.4067	8.4118	8.4157	8.4207	8.4265	8.4416
Cell volume V (Å^3)	594.13	595.21	596.03	597.1	598.34	601.59
Hopping length L_A (Å)	3.6402	3.6424	3.6441	3.6463	3.6488	3.6553
Hopping length L_B (Å)	2.9722	2.974	2.9754	2.9772	2.9792	2.9846
Bond Length A-O (Å)	1.8201	1.8212	1.822	1.8231	1.8244	1.8277
Bond length A-B (Å)	2.1017	2.103	2.1039	2.1052	2.1066	2.1104
Ionic Radii r_A (Å)	0.4701	0.4713	0.472	0.4731	0.4744	0.4777
Ionic Radii r_B (Å)	0.7516	0.753	0.7539	0.7552	0.7566	0.7604
X-ray density Δx (gr/cm^3)	5.3422	5.428	5.516	5.6012	5.6847	5.7492

Table 2 – The values of Crystallite size (D) and Lattice strain (ε) calculated by Scherrer's method, W-H method and SSP method

$Co_{1-x}Cd_xFe_2O_4$ content, (x)	Scherrer Method		W-H Method		SSP Method	
	Crystallite size (D)	Microstrain (ε)	Crystallite size (D)	Microstrain (ε)	Crystallite size (D)	Microstrain (ε)
0.08	175	0.001992	164	0.00058	155	0.01165
0.16	192	0.001819	194	0.000513	164	0.0121
0.24	229	0.001537	235	0.000503	186	0.01203
0.32	271	0.001297	256	0.00048	214	0.01113
0.40	341	0.001041	291	0.000445	244	0.01075
0.48	378	0.000936	398	0.0004	278	0.00925

4. CONCLUSIONS

In this study, we investigated the effect of Cd^{2+} subsituation on the structural properties of $Co_{1-x}Cd_xFe_2O_4$ nanoparticles through X-ray analysis. The co-precipitation method was successfully used to synthesis nano powder of $Co_{1-x}Cd_xFe_2O_4$ ferrite. A small increase was found in lattice constant (8.4067 to 8.4416 Å) because of the larger ionic radii of Cd^{2+} ions as compared to Co^{2+} ions. Here, several methods were used for determine the structural properties of Cd doped cobalt ferrite nanoparticles. The analysis of each method revealed that the crystallite size was increased with increase of Cd concentration while strain was decreased with increase of Cd content.

REFERENCES

1. B. Cantor, *Novel Nanocrystalline Alloys and Magnetic Nanomaterials* (Taylor and Francis Ltd: 2019).
2. F. Huixia, C. Baiyi, Z. Deyi, Z. Jianqiang, T. Lin, *J. Magn. Magn. Mater.* **356**, 68 (2014).
3. S.I. Ahmad, *J. Magn. Magn. Mater.* **562**, 169840 (2022).
4. M.K. Rendale, S.N. Mathad, V. Puri, *Microelectron. Int.* **34** No 2, 57 (2017).
5. A.S. Pujar, A.B. Kulkarni, S.N. Mathad, et al., *Int. J. Self-Propagating High-Temperature Synthesis* **27**, 174 (2018).
6. M.R. Patil, M.K. Rendale, S.N. Mathad, R.B. Pujar, *Inorg. Nano-Metal Chem.* **47** No 8, 1145 (2017).
7. A.B. Kulkarni, S.R. Manohara, R. Vishwaroop, S.N. Mathad, *Macromolecular Symposia* **400**, 2100113 (2021).
8. R.M. Shedam, P.P. Kashid, S.N. Mathad, *J. Nano- Electron. Phys.* **14** No 4, 04001 (2022).
9. M. Maashani, K. Khalaf, A. Gismelseed, I. Al-Omari, *J. Alloy. Compd.* **817**, 152786 (2020).
10. R. Kulshrestha, V. Anand, *Int. J.* **8**, 207 (2019).
11. A. Pirouzfar, S.A. Seyyed Ebrahimi, *J. Magn. Magn. Mater.* **370**, 1 (2014).
12. A.S. Pujar, A.B. Kulkarni, S.N. Mathad, et al., *Int. J Self-Propag. High-Temp. Synth.* **27**, 174 (2018).
13. V.P. Senthil, J. Gajedriran, S. Gokul Raj, T. Shanmugavel, G. Ramesh Kumar, C.P. Reddy, *J. Chem. Phys. Lett.* **695**, 19 (2018).
14. Ch. Reddy, C. Byon, B. Narendra, D. Baskar, G. Srinivas, Jaesool Shim, S.V. Prabhakar Vattikuti, *Superlattice. Microstruct.* **82**, 165 (2015).
15. A.M. Abdeen, O.M. Hemeda, E.E. Assem, M.M. El-Sehly, *J. Magn. Magn. Mater.* **238** No 1, 75 (2002).
16. H. Shashidharagowda, S.N. Mathad, *Mater. Sci. Eng. Technol.* **3**, 201 (2020).
17. R.P. Patil, S.B. Patil, B.V. Jadhav, S.D. Delekar, P.P. Hankare, *J. Magn. Magn. Mater.* **401**, 870 (2016).
18. A.M.M. Farea, S. Kumar, K.M. Batoo, A. Yousef, C.G. Lee, Alimuddin, *J. Alloy. Compd.* **464**, 361 (2008).
19. A.B. Kulkarni, S.N. Mathad, *Sci. Sinter.* **53**, 407 (2021).
20. V.D. Mote, Y. Purushotham, B.N. Dole, *J. Theor. Appl. Phys.* **6**, 6 (2012).
21. Heryanto, B. Abdullah, D. Tahir, Mahdalia, *J. Phys. Conf. Ser.* **1317**, 012052 (2019).

Синтез і дослідження структури наночастинок фериту кобальту легованих кадмієм за допомогою рентгенівського дифракційного аналізу

Priyanka P. Kashid[1,2], Shridhar N. Mathad[1,2], Rakesh M. Shedam[1,2], Mahadev Shedam[3]

[1] *Department of Engineering Physics, K.L.E. Institute of Technology, Gokul Road, Hubballi, 580027 Karnataka, India*
[2] *Visvesvaraya Technological University (VTU), 590018 Belagavi, India*
[3] *The New College, Kolhapur, India*

У цій роботі досліджено структурні властивості нанокристалічних наночастинок фериту кобальту ($Co_{1-x}Cd_xFe_2O_4$), легованого Cd^{2+}, синтезованих методом співосадження. Рентгеноструктурне дослідження знову виявило утворення монофазних кубічних шпінелей. Виявлено збільшення розміру кристалітів від 17 до 38 нм зі збільшенням концентрації кадмію. Інші структурні параметри, такі як стала гратки (a), об'єм (V), довжини стрибків (L_A і L_B), довжини зв'язків (A-O і B-O), іонні радіуси (r_A і r_B), щільність рентгенівського випромінювання (D_x), мікродеформація (ε) та щільність дислокацій (ρ_D). Тут використовувалися методи W-H і Size-Strain Plot для отримання значень деформації решітки та розміру кристалітів з аналізу розширення піків рентгенівської дифракції. Кожен метод аналізу давав різні результати, оскільки розбіжності були виявлені в обчислених параметрах.

Ключові слова: Мікродеформація (ε), Розмір кристаліту (D), Щільність рентгенівського випромінювання (D_x), Наночастинки фериту, Заміщення Cd^{2+}.